Finite-size effects in the conductance and giant magnetoresistance of Fe/Cr and Co/Cu nanowires

Julian Velev and Yia-Chung Chang
Department of Physics and Materials Research Laboratory, University of Illinois at Urbana-Champaign, Urbana, Illinois 61801
(Received 1 October 2002; revised manuscript received 16 January 2003; published 29 April 2003)

We present theoretical studies of the size dependence of the current perpendicular-to-the-plane ballistic conductance and giant magnetoresistance (GMR) in Fe/Cr and Co/Cu nanowires within a realistic tight-binding model. Symmetry properties of the nanowire with respect to transformations of the point group C_{4v} are exploited to decompose the problem into several independent parts. This allows us to study mesoscopic-size nanowires which are experimentally achievable. Our calculations predict substantial reduction in GMR due to the finite size of the nanowire.

DOI: 10.1103/PhysRevB.67.144425 PACS number(s): 73.23.−b, 75.70.−i

I. INTRODUCTION

In the decade after the discovery of the giant magnetoresistance (GMR) in Fe/Cr multilayers,[1,2] the field has received a lot of attention.[3–7] One of the recent developments in this field is the study of multilayered nanowires.[8–10] These systems have shown high current-perpendicular-to-the-plane (CPP) GMR ratios with substantial resistances because the dimension of their cross sections is comparable with their length (see Ref. 11).

The typical magnetic nanowire system is cylindrical with a diameter as small as 10 nm. The nanowire consists of alternating magnetic and nonmagnetic slices each of thickness on the order of 3–20 nm. The total length of the nanowire is on the order of microns. Due to the shape anisothropy, the preferred direction of magnetization is along the axis of the nanowire. Furthermore, the small thickness of the spacer layer allows an interaction between the magnetic layers which favors ferromagnetic coupling. So the contribution to GMR comes from a relatively small number of surfaces which are antiferromagnetically coupled in the absence of an external magnetic field.

In a previous work,[12] we reported studies of GMR in small Fe/Cr nanowires within a realistic tight-binding model. Our results showed a diminished value of GMR due to the uneven suppression of the two spin channels which we attributed to the finite size of the nanowire. In this article we study the size dependence of GMR for both Fe/Cr and Cu/Co nanowires with dimensions ranging from the atomic scale to the mesoscopic scale, which was previously unattainable. This is accomplished by exploiting the symmetry of the wire to decompose the problem into several disconnected problems for wave functions associated with different symmetry types. Furthermore, we introduce a recursive scheme to invert the Hamiltonian matrix efficiently (see the Appendix). This allows us to study supercells that are more than 6 times larger than those studied previously.

II. MODEL

The method we use to calculate the conductance has been described in detail elsewhere.[13,14] For a multilayer sandwiched between two leads at zero temperature, the conductance is given by[15]

$$\Gamma = \frac{e^2}{h}\mathrm{Tr}[\tilde{\Sigma}_L G^R(1,n)\tilde{\Sigma}_R G^A(1,n)], \tag{1}$$

where $G^{R/A}(1,n)$ is the retarded/advanced Green's function (GF) matrix element between the first and last principal layers of the sample and $\tilde{\Sigma} = i(\Sigma^R - \Sigma^A)$ is the imaginary part of the self-energy associated with the leads. In the calculation of the conductance, all Green's functions and self-energies are evaluated at the Fermi energy.

We model the nanowires with a square supercell within the tight-binding (TB) formalism. In order to decouple the neighboring nanowires, we surround the wire with empty sites. The supercell is repeated periodically in the plane. The obtained superlattice has a square lattice with lattice constant $L = Na$, where a is the bulk lattice constant and N is an integer, which indicates the size of the supercell.

The wave functions of the system can be written in terms of linear combinations of *supercell orbitals* defined as

$$|\mathbf{k}+\mathbf{g}_n, i, \alpha, R_z\rangle = \frac{1}{N}\sum_{\bar{\mathbf{R}}_s} e^{i(\mathbf{k}+\mathbf{g}_n)\cdot\bar{\mathbf{R}}_s}|\alpha, \mathbf{R}_s+\mathbf{S}_i\rangle, \tag{2}$$

where $\mathbf{k}=(k_x,k_y)$ $(|k_x|,|k_y|<\pi/L)$ denotes a two-dimensional (2D) wave vector within the superlattice Brillouin zone (BZ), α labels the symmetry type for the sp^3d^5 orbitals, $\bar{\mathbf{R}}_s$ denotes the projection of the superlattice lattice vector $\mathbf{R}_s$ on the (x,y) plane located at R_z, $\mathbf{S}_i$ label the atom coordinates in the supercell, and $\mathbf{g}_n=(2\pi/L)(n_1,n_2)$ denotes the reciprocal lattice vectors of the superlattice that fall in the first bulk Brillouin zone $(0\leqslant n_1,n_2\leqslant N)$.

In the supercell orbital basis, the Hamiltonian matrix element is

$$H_{ij,\alpha\beta}(\mathbf{k}) = \sum_{\bar{\mathbf{R}}_s} e^{i(\mathbf{g}_n+\mathbf{k})\cdot\bar{\mathbf{R}}_s}\langle\alpha, \mathbf{S}_i|H|\beta, \mathbf{R}_s+\mathbf{S}_j\rangle, \tag{3}$$

and the Green's function for the semi-infinite leads is

$$G_{ij}(\mathbf{k}) = \frac{1}{N^2}\sum_n e^{i(\mathbf{g}_n+\mathbf{k})\cdot(\mathbf{S}_i-\mathbf{S}_j)}G(\mathbf{g}_n+\mathbf{k}). \tag{4}$$

Here the labels α and R_z have been omitted for brevity. Due to translational symmetry, the layer orbitals associated with

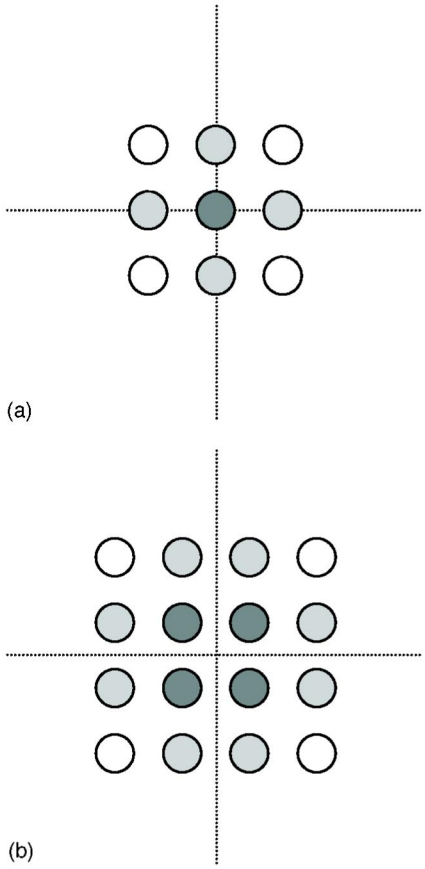

FIG. 1. Schematic plots of the cross sections of supercells with C_{4v} point symmetry with an (a) odd number and (b) even number of unit cells.

different wave vectors $\mathbf{g}_n$ are decoupled in the leads, but coupled in the nanowire region.

III. REDUCTION VIA SYMMETRIZATION

In the study of conductance and GMR in nanowires of realistic sizes, large supercells are needed. The symmetry of the supercell allows substantial reduction of the problem to be achieved using group theory. As the size of the nanowire increases, the supercell BZ becomes so small that a single-point sampling (chosen to be $\mathbf{k}_\parallel = 0$) is sufficient for getting an accurate result. In this case, there is no phase change in going from one unit cell to another. Thus, we can exploit the full point-group symmetry of the system. Let us consider a shell of atoms, which are at an equal distance from the center: i.e., the set of orbitals $\{|\alpha, \mathbf{S}_i\rangle: |\mathbf{S}_i| = \text{const}\}$. In Fig. 1(a), a symmetric supercell with an odd number of unit cells is shown. The atoms that are equally distant from the center form shells that are differently shaded. Figure 1(b) shows a similar supercell with an even number of unit cells. The cross section of both bcc and fcc lattices in (001) orientation is a square lattice which breaks down in only a few topologically different shells. The four topologically different shells with their symmetry states are shown in Fig. 2. The point group considered here is C_{4v}, which contains eight elements

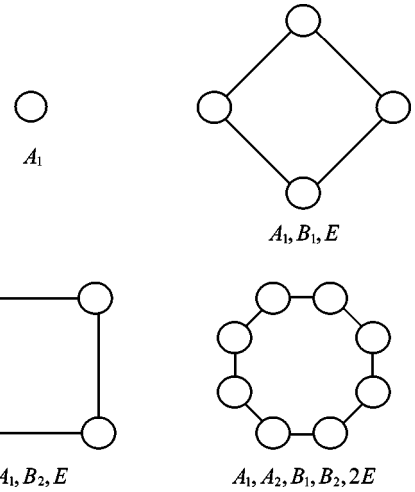

FIG. 2. Topologically different shells in cross section of the bcc (001) supercell.

and it has four 1D (A_1, A_2, B_1, and B_2) and one 2D (E) irreducible representations.[16]

Let R label the symmetry operations in C_{4v}. We first construct the site functions that transform according to the different rows of the different irreducible representations (IR's) of C_{4v} by using the projection operator defined as

$$\mathcal{P}^{(n)}_{\nu'\nu} = \frac{l_n}{h} \sum_R \Gamma^{(n)}(R)^*_{\nu'\nu} R, \tag{5}$$

where l_n is the dimensionality of the nth representation, h the dimensionality of the group, and $\Gamma^{(n)}(R)_{\nu'\nu}$ denotes the matrix element of the IR corresponding to group element R. Starting with an arbitrary site function $|\mathbf{S}\rangle$ in a given shell, we then obtain symmetrized shell orbitals given by $\mathcal{P}^{(n)}_{\nu\nu}|\mathbf{S}\rangle$. For multidimensional representations one can obtain the functions transforming according to other rows of the same representation by applying the off-diagonal projection operator $\mathcal{P}^{(n)}_{\nu'\nu}$. In our case, E is the only multidimensional representation, but since the directions x and y are physically equivalent, we can consider only part of the E symmetry (say, x) and the second part will automatically give the same result.

Next, we construct symmetrized tight-binding basis functions that transform according to various IR's of C_{4v}. The atomic orbitals are denoted by $\alpha = s, x, y, z$ (p like) or $xy, yz, zx, (x^2-y^2), (3z^2-r^2)$ (d like). These orbitals transform according to the various IR's of C_{4v} as given in Table I. The overall linear combination of atomic orbitals (LCAO), written as a product of a shell orbital transforming according to $\Gamma^{(n)}$ and angular part transforming according to $\Gamma^{(m)}$, transforms according to the direct-product representation

TABLE I. Symmetry character of the atomic orbitals.

s	(x,y)	z	xy	(zx,yz)	x^2-y^2	$3z^2-r^2$
A_1	E	A_1	B_2	E	B_1	A_1

TABLE II. Multiplication table of the irreducible representations of C_{4v} ($A_1 \equiv \Gamma_1$, $A_2 \equiv \Gamma_2$, $B_1 \equiv \Gamma_3$, $B_2 \equiv \Gamma_4$, and $E \equiv \Gamma_5$).

	Γ_1	Γ_2	Γ_3	Γ_4	Γ_5
Γ_1	Γ_1	Γ_2	Γ_3	Γ_4	Γ_5
Γ_2		Γ_1	Γ_4	Γ_3	Γ_5
Γ_3			Γ_1	Γ_2	Γ_5
Γ_4				Γ_1	Γ_5
Γ_5					$\Gamma_1+\Gamma_2+\Gamma_3+\Gamma_4$

$\Gamma^{(n)}\Gamma^{(m)}$. Since these are representations of the same group, the direct-product representation must be reducible:

$$\Gamma^{(i)}\Gamma^{(j)} = \sum_k a_{ijk}\Gamma^{(k)}. \tag{6}$$

Using the vector-coupling coefficients[17] as given in Table II, we can then obtain symmetried LCAO in the form

$$\psi_\nu^{(n)} = \sum_{\alpha,i} T_{\alpha,i}^{(n,\nu)} |\alpha, \mathbf{S}_i\rangle.$$

Finally, the Hamiltonian is block diagonalized within the basis of symmetrized LCAO via the transformation

$$H^{n\nu} = (T^{(n\nu)})^\dagger \cdot H \cdot T^{(n\nu)} \tag{7}$$

and we can solve for the A_1, A_2, B_1, B_2, and E_x symmetries separately. The total conductance (Γ) can be decomposed into contributions from various symmetry channels in the form

$$\Gamma = \sum_n \sum_{\nu=1}^{l_n} \Gamma^{(n\nu)}. \tag{8}$$

IV. RESULTS AND DISCUSSIONS

We study the GMR effect in Fe/Cr and Co/Cu nanowires with size ranging from atomic scale to mesoscopic scale. To take advantage of the symmetry, we choose nanowires which are invariant under fourfold rotations about the z axis. Our calculations show that for nanowires with cross section above a certain size N_c, the single-**k**-point ($\mathbf{k}_\parallel = 0$) sampling in the surface Brillouin zone gives results in very good agreement with those obtained with zone integration. Below N_c, we calculate the conductance without utilizing symmetry by integrating over the surface Brillouin zone. For sizes above N_c, we utilize the point-group symmetry and decompose the total conductance into contributions from various symmetry channels.

Figure 3(a) shows the conductance versus the size (N) of the supercell in an $N \times N$ Fe(4)/Cr(3)/Fe(4) nanowire obtained using this method. Here the notation Fe(4)/Cr(3)/Fe(4) stands for a trilayer consisting of 4 ml Fe, 3 ml Cr, and 4 ml Fe, sandwiched between semi-infinite Cr leads. The conductance is normalized with respect to the conductance of a multilayer of the same geometry, which is 0.20 (0.88) e^2/h for majority (minority) in parallel configuration and 0.20 e^2/h for either channel in antiparallel configuration. At small

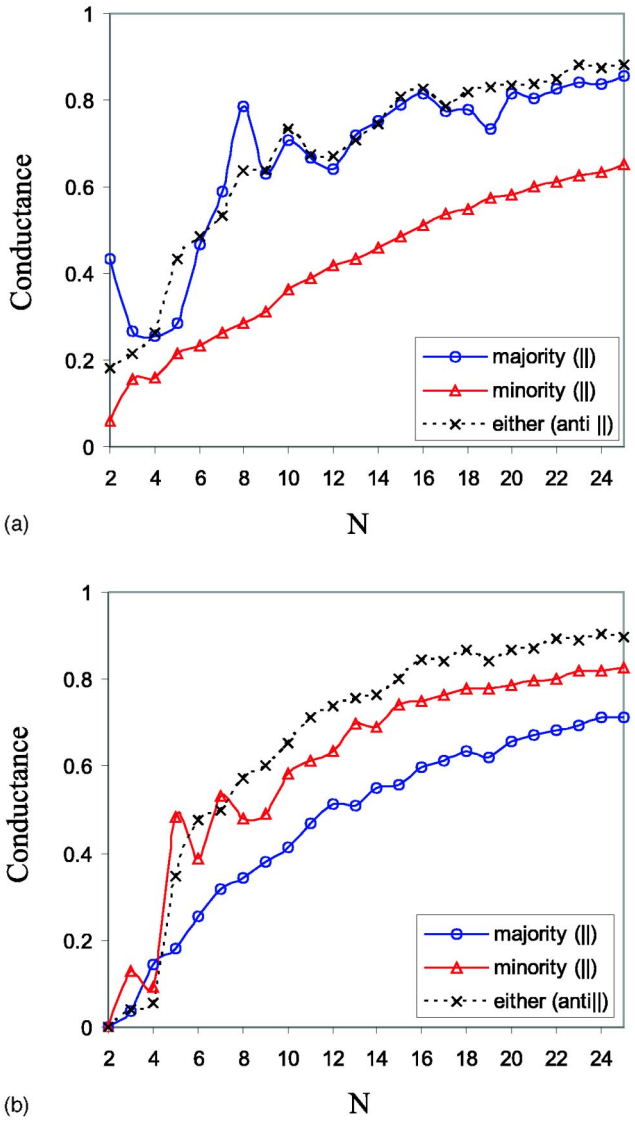

FIG. 3. Conductance vs size (N) for $N \times N$ (a) Fe(4)/Cr(3)/Fe(4) and (b) Co(4)/Cu(3)/Co(4) nanowires.

sizes the conductance of the minority channel is very small and it increases steadily throughout as the size increases. The majority channel, on the contrary, starts higher and its conductance increases fast to about 70% of the multilayer conductance after which its slope becomes comparable to the slope of the minority conductance. Figure 3(b) shows the conductance versus the size of the supercell in an $N \times N$ Co(4)/Cu(3)/Co(4) nanowire. The conductance is normalized to the conductance of a multilayer of the same geometry, which is 1.25 (0.61) e^2/h for majority (minority) in parallel configuration and 0.54 e^2/h for either channel in antiparallel configuration. Overall, the behavior is very similar to the case of Fe/Cr, the difference in behavior between corresponding spin channels in Fe/Cr and Co/Cu originating from the band structure of the nonmagnetic material. In Cr, the d bands are partially occupied, whereas in Cu, the d bands are almost filled. Therefore, the transport in Fe/Cr is due to both s and d electrons while in Co/Cu it is almost entirely from s

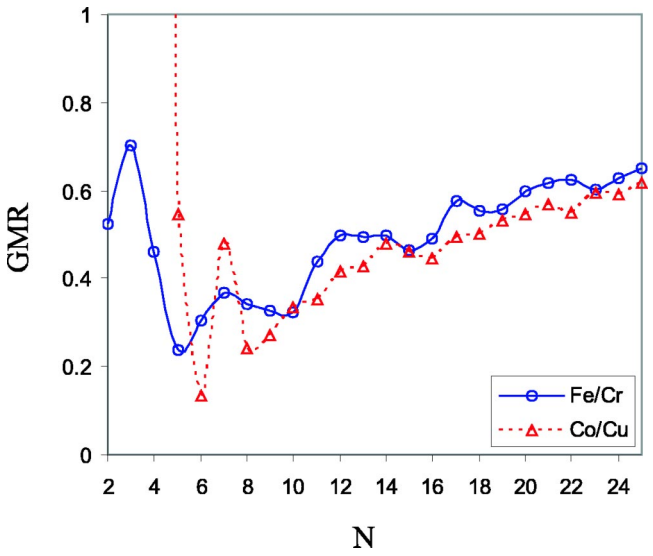

FIG. 4. GMR vs size (N) for $N\times N$ Fe(4)/Cr(3)/Fe(4) and (Co(4)/Cu(3)/Co(4) nanowires.

electrons. Thus, in the conceptually simpler case of Co/Cu, the ''geometrical'' resistance is proportional to how much the density of states (DOS) for the *s* band differs from the bulk. For that reason, the geometrical resistance is the same for all channels. In the case of Fe/Cr, the minority and majority channels are very different. In the minority channel, the conductance is predominantly due to *s* electrons due to their high mobility. The *s* electron DOS is strongly affected by the confinement, which causes large band mismatch between the lead and wire. In the majority channel, due to the band mismatch and the *s*-*d* hybridization, a significant portion of the conductance comes from the *d* electrons. Due to their localized character, they are much less affected by the confinement. As a result the majority conductance increases sharply with the increase of size. For very small sizes, however, the *d* component DOS is already very close to its bulk counterpart. Thus, the main source of geometrical resistance is from the DOS of the *s* electrons. This is nicely illustrated by the change of slope in the majority conductance graph.

GMR versus the size of the supercell in an $N\times N$ Fe(4)/Cr(3)/Fe(4) and Co(4)/Cu(3)/Co(4) nanowires is shown in Fig. 4. Here the nanowire GMR is normalized with respect to the GMR of a multilayer of the same layer arrangement, which is 161% (74%) for the Fe/Cr (Co/Cu). This figure illustrates the main point in this study: namely, that the value of the useful property of these multilayered nanowires can be greatly depreciated due to the finite size (for cross sections larger than a few atoms). GMR increases slowly with the size and it is about 65% of the multilayer value in this Fe/Cr nanowire with diameter more than 7 nm. The maximum value of GMR we obtained for the Co/Cu nanowire is 62% of the multilayer value. On the other hand, the peak in GMR for atomic-size nanowires (essentially nanocontacts) demonstrates possibilities for huge GMR ratios. The effect is much more pronounced in Co/Cu where the nanowire with a four-atom cross section shows GMR 20 times larger than the corresponding multilayer. The problem of nanocontacts, however, is beyond of the scope of this study.

V. CONCLUSION

We have developed a method to study the ballistic conductance in nanowires with atomic-size to medium-size cross sections. We take full advantage of the point-group symmetry of the system to reduce the computational effort of the problem for larger cross sections. We find that in this range of sizes the ''geometrical'' resistance, arising from the lateral confinement, is the leading source of resistance. The dispersive *s* bands are more affected by the confinement. They determine the geometrical resistance completely in nanowires with cross sections larger than few unit cells . The nondispersive *d* bands are affected by the confinement only at very small sizes. They determine the conductance of the large-band-mismatch channels in which *s*-*d* hybridization is important. This has important practical consequences: namely, GMR can be substantially decreased in nanowires as compared to multilayers due to the uneven suppression of the different spin channels. Thus, the effort to make the nanowires smaller can be counterproductive beyond a certain limit.

ACKNOWLEDGMENTS

This work was supported in part by DARPA, Grant No. DAAD19-01-1-0324, and by the MURI program, ARL, Contract No. DAAD19-01-1-0591.

APPENDIX RECURSIVE INVERSION

In the Landauer formula for calculating the conductance all we need is the Green's function matrix element between the first layer and last principal layer (PL) of the sample. A PL is defined as a minimum set of atom planes such that the interaction between atomic orbitals located in any two nonadjacent PL's is zero. One way to obtain it is to construct the Hamiltonian matrix of the sample and partially invert it. This method requires storing a matrix, the size of which increases linearly with the size of the nanowire (if we take into account the fact that every layer sees only a fixed number of neighboring layers). Another way to obtain the GF matrix element is to express it recursively in terms of the Hamiltonian matrix elements in two adjacent PL's.

The system can be divided into three parts: the left lead, the nanowire slab, and the right lead. The corresponding GF's are denoted by G_L, G_S, and G_R, respectively. To connect the nanowire slab to the infinite leads, we have to define TB matrix elements in the interface region. As in typical empirical TB calculations, we take them to be the arithmetic average of the hopping integrals associated with the constituent materials on both sides of the interface. The matrix equation for the full GF of the system takes the form

$$\begin{pmatrix} G_L & G_{LS} & G_{LR} \\ G_{SL} & G_S & G_{SR} \\ G_{RL} & G_{RS} & G_R \end{pmatrix} = \begin{pmatrix} E-H_L & -H_{LS} & 0 \\ -H_{SL} & E-H_S & -H_{SR} \\ 0 & -H_{RS} & E-H_R \end{pmatrix}^{-1}. \tag{A1}$$

If we do the inversion analytically, we can obtain the GF associated with the nanowire slab in terms of the self-energies which take into account the effects of coupling with the leads,

$$G_S=(E-H_S-\Sigma_L-\Sigma_R)^{-1}, \tag{A2}$$

where the self-energies have the form

$$\Sigma_L=H_{SL}G_LH_{LS},$$

$$\Sigma_R=H_{SR}G_RH_{RS}. \tag{A3}$$

We notice that the self-energies are actually small matrices, because, by definition, there is overlap only between the last principal layer of the lead and the first principal layer of the nanowire.

We can invert the matrix $A_S\equiv E-H_S-\Sigma_L-\Sigma_R$ explicitly written in the form

$$\begin{pmatrix} A_{11} & A_{12} & 0 \\ A_{21} & A_{22} & A_{23} \\ 0 & A_{32} & A_{33} \end{pmatrix}\begin{pmatrix} G_{11} & G_{12} & G_{13} \\ G_{21} & G_{22} & G_{23} \\ G_{31} & G_{32} & G_{33} \end{pmatrix}=\begin{pmatrix} 1 & 0 & 0 \\ 0 & 1 & 0 \\ 0 & 0 & 1 \end{pmatrix}, \tag{A4}$$

which is partitioned such that $A_{11}=E-H_{11}-\Sigma_L$ and $A_{33}=E-H_{33}-\Sigma_R$ contain only matrix elements within one PL (for the end layers of the nanowire) and A_{22} contains the matrix elements for the rest of the nanowire. At any given time the middle block has to be larger than 1 PL in order for the overlap between the first and the last PL's to be zero. The GF matrix element G_{31} is obtained to be

$$G_{31}=A_{33}^{-1}A_{32}(A_{22}-A_{21}A_{11}^{-1}A_{12}-A_{23}A_{33}^{-1}A_{32})^{-1}A_{21}A_{11}^{-1}. \tag{A5}$$

Note also the special structure of the overlap matrices. Since the PL is defined such that it sees only one PL to the left and one to the right, the matrices A_{ij} $(i\neq j)$ are mostly zero:

$$A_{12}=\begin{pmatrix} -H_{1,2} & 0 & \cdots & 0 \end{pmatrix},$$

$$A_{32}=\begin{pmatrix} 0 & \cdots & 0 & -H_{n,n-1} \end{pmatrix}, \tag{A6}$$

where $H_{1,2}$ is the overlap matrix element between the first and second PL's of the sample and $H_{n,n-1}$ between the last one and the one before the last. This implies that we can use the self-energy to absorb the effect of coupling between the middle part of the slab to the end layers recursively, each time reducing the size of the A matrix by 2 PL's. We write, after n recursive steps,

$$A^{(n+1)}=A_{22}^{(n)}-\Sigma_L^{(n+1)}-\Sigma_R^{(n+1)}, \tag{A7}$$

where

$$\Sigma_L^{(n+1)}=A_{21}^{(n)}(A_{11}^{(n)})^{-1}A_{12}^{(n)}, \tag{A8}$$

$$\Sigma_R^{(n+1)}=A_{23}^{(n)}(A_{33}^{(n)})^{-1}A_{32}^{(n)} \tag{A9}$$

are the new self-energies. This procedure can continue until the size of the matrix $A^{(n+1)}$ is reduced to a point at which it cannot be reduced more without introducing overlap between the first and the last PL's. At this point, it is inverted directly. The algorithm can be implemented iteratively by storing the partial result of the matrix multiplications to the left and right.

There are several advantages to this approach—first, one does not need to store the Hamiltonian of the whole sample but only the parts currently needed for the calculation; second, the memory requirements are independent of the length of the wire; last, all matrix operations are performed on fixed-size matrices.

[1] M.N. Baibich, J.M. Broto, A. Fert, F. Nguyen Van Dau, F. Petroff, P. Etienne, G. Creuzet, A. Friederich, and J. Chazelas, Phys. Rev. Lett. **61**, 2472 (1988).

[2] G. Binasch, P. Grunberg, F. Saurenbach, and W. Zinn, Phys. Rev. B **39**, 4828 (1989).

[3] P.M. Levy, Solid State Phys. **47**, 367 (1994).

[4] M. Gijs and G. Bauer, Adv. Phys. **46**, 285 (1997).

[5] E.Y. Tsymbal and D.G. Pettifor, Solid State Phys. **56**, 113 (2001)

[6] J. Bras and W.P. Pratt, J. Magn. Magn. Mater. **200**, 274 (1999).

[7] *Magnetic Multilayers and Giant Magnetoresistance: Fundamentals and Industrial Applications*, edited by U. Hartmann (Springer, Berlin, 2000).

[8] A. Blondel, J.P. Meir, B. Doudin, and J.-Ph. Ansermet, Appl. Phys. Lett. **65**, 3019 (1994).

[9] K. Liu, K. Nagodawithana, P.C. Pearson, and C.L. Chien, Phys. Rev. B **51**, 7381 (1995).

[10] L. Piraux, J.M. George, J.F. Despres, C. Leroy, E. Ferain, R. Legras, K. Ounadjela, and A. Fert, Appl. Phys. Lett. **65**, 2484 (1994).

[11] A. Fert and L. Pireaux, J. Magn. Magn. Mater. **200**, 338 (1999).

[12] J. Velev and Y.C. Chang, J. Magn. Magn. Mater. **250C**, 219 (2002).

[13] J. Velev and Y.C. Chang, Phys. Rev. B **63**, 184411 (2001).

[14] J. Velev and Y.C. Chang, Phys. Rev. B **64**, 104404 (2001).

[15] S. Datta, *Electronic Transport in Mesoscopic Systems* (Cambridge University Press, Cambridge, England, 1997).

[16] M. Tinkham, *Group Theory and Quantum Mechanics* (McGraw-Hill, New York, 1964).

[17] G. Koster, J. Dimmock, R. Wheeler, and H. Statz *Properties of the Thirty-Two Point Groups* (MIT Press, Cambridge, MA, 1963).